



Preservation of shortening velocity and power output in single muscle fibres from patients with idiopathic inflammatory myopathies

Franco Henning^{1,2} · Tertius Abraham Kohn^{2,3}

Received: 10 July 2022 / Accepted: 5 December 2022 / Published online: 15 December 2022
© The Author(s), under exclusive licence to Springer Nature Switzerland AG 2022

Abstract

Idiopathic inflammatory myopathies (IIMs) are autoimmune disorders of skeletal muscle causing weakness and disability. Utilizing single fibre contractility studies, we have previously shown that contractility is affected in muscle fibres from individuals with IIMs. For the current study, we hypothesized that a compensatory increase in shortening velocity occurs in muscle fibres from individuals with IIMs in an effort to maintain power output. We performed in vitro single fibre contractility studies to assess force–velocity relationships and maximum shortening velocity (V_{\max}) of muscle fibres from individuals with IIMs (25 type I and 58 type IIA) and healthy controls (66 type I and 27 type IIA) and calculated maximum power output (W_{\max}) for each fibre. We found significantly higher V_{\max} (mean \pm SEM) of fibres from individuals with IIMs, for both type I (1.40 ± 0.31 fibre lengths/s, $n = 25$ vs. 0.63 ± 0.13 fibre lengths/s; $p = 0.0019$) and type IIA fibres (2.00 ± 0.17 fibre lengths/s vs. 0.77 ± 0.10 fibre lengths/s; $p < 0.0001$). Furthermore, W_{\max} (mean \pm SEM) was maintained compared to fibres from healthy controls, again for both type I and type IIA fibres (4.10 ± 1.00 kN/m²·fibre lengths/s vs. 2.00 ± 0.16 kN/m²·fibre lengths/s; $p = \text{ns}$ and 9.00 ± 0.64 kN/m²·fibre lengths/s vs. 6.00 ± 0.67 kN/m²·fibre lengths/s; $p = \text{ns}$ respectively). In addition, type I muscle fibres from individuals with IIMs was able to develop maximum power output at lower relative force. The findings of this study suggest that compensatory responses to maintain power output, including increased maximum shortening velocity and improved efficiency, may occur in muscle of individuals with IIMs. The mechanism underlying this response is unclear, and different hypotheses are discussed.

Keywords Skeletal muscle · Inflammatory myopathies · Single fibre contractility · Maximum shortening velocity

Introduction

Idiopathic inflammatory myopathies (IIMs) are autoimmune disorders of skeletal muscle, affecting individuals of all ages, and usually present as subacute onset of symmetric proximal and axial weakness and fatigue (Dalakas and Hohlfeld 2003; Mastaglia et al. 2003; Kluger et al. 2013). Although different entities are recognized within this group of disorders,

including dermatomyositis, polymyositis, necrotizing autoimmune myopathy, and inclusion-body myositis, most of them share certain core features. These include symmetrical proximal and axial weakness, subacute course, elevated serum muscle enzymes (creatinine kinase), inflammation, necrosis, and regeneration on muscle histology, myopathic features and “irritable” phenomena on electrophysiological examination, and responsiveness to immunosuppressive therapy. In contrast to many hereditary myopathies, where abnormal or dysfunctional proteins may lead to impaired muscle fibre contractility (Fink et al. 1990; Krivickas et al. 2000; Lassche et al. 2013), the mechanism of weakness in IIMs is less clear. We previously performed permeabilized single muscle fibre contractility studies on muscle biopsies from individuals with IIMs and healthy controls and found impaired normalised contractile force production in the IIM group (Henning and Kohn 2020). Absolute force and specific force (force normalised to cross-sectional area) of type I fibres were 42% and 30% lower in the IIMs group, whereas

✉ Franco Henning
fhenning@sun.ac.za

¹ Division of Neurology, Department of Medicine, Faculty of Medicine and Health Sciences, Stellenbosch University, Cape Town, South Africa

² Department of Human Biology, University of Cape Town, Anzio Road, Observatory, Cape Town, South Africa

³ Department of Medical Bioscience, Faculty of Natural Sciences, University of the Western Cape, Cape Town, South Africa

absolute and specific force of type IIA fibres were 16% and 35% lower (Fig. 1). This finding suggests that weakness in IIMs may, at least in part, be caused by dysfunction of the contractile apparatus, and has also been illustrated in mouse models (Coley et al. 2012; Himori et al. 2021).

If this is indeed the case, a question arises over which, if any, compensatory changes occur in muscle fibres in order to maintain power output in the presence of decreased force generating capacity. Since $power = force \times velocity$, maintenance of power output would require an increase in shortening velocity as contractile force decreases. A single previous study compared maximal unloaded shortening velocity of muscle fibres from individuals with dermatomyositis and healthy controls, and found this to be 33% higher in type I fibres from individuals with dermatomyositis, while no difference was found in type IIA fibres (Krivickas et al. 2005). The authors hypothesised that this may be a compensatory mechanism to maintain muscle power output in the face of loss of force producing capacity, which arose from muscle fibre atrophy. However, it should be noted that, in this previous study, single fibre maximal and specific force production in dermatomyositis was not decreased compared to healthy controls (it was in fact significantly higher), and therefore the increased shortening velocity should not necessarily be regarded as a compensatory mechanism. This study also had some shortcomings: firstly, the biopsied muscles in individuals with dermatomyositis were either of normal strength or only mildly weak, and secondly, not all biopsies were taken from the same muscle (all control biopsies were from the *vastus lateralis* muscle, while dermatomyositis biopsies were from the *biceps* or *deltoid* muscles).

In order to determine maximum shortening velocity, conditions of zero load need to be recreated or simulated. Two main techniques have been described, namely the slack test and the

force clamp test. The slack test was first described by Edman (1979) and is performed by rapidly releasing the tension to zero during a contraction and measuring the time to the start of tension redevelopment (Edman 1979). This is repeated at different magnitudes of release, and the slope of the relation between size of the release and measured time represents the steady state shortening velocity at zero load (unloaded shortening velocity, V_0), which is different from maximum shortening velocity at zero load (V_{max}) (Bottinelli and Reggiani 2000). V_{max} is derived from the force–velocity curve by extrapolation of shortening velocities obtained at various pre-determined isotonic force tests (force clamps). This relation between force and shortening velocity, first characterised by Hill (1938), can be illustrated as part of a rectangular hyperbola, described by the equation $(P + a)(V + b) = (P_0 + a)b$, where P is the force during shortening at velocity V , P_0 is the force during an isometric contraction, and a and b are constants (Hill 1938). The curvature of the hyperbola is given by the value of a/P_0 . According to Bottinelli and Reggiani (2000), determining V_{max} using force clamps provides more information about the contractile properties of a single fibre, especially to aid in constructing force–velocity curves, maximum power generation and the optimum force to achieve maximum power, whereas the slack test does not (Bottinelli and Reggiani 2000). The difference between V_0 and V_{max} is not significant in slow twitch fibres, but V_0 is significantly greater than V_{max} in fast twitch fibres (Bottinelli et al. 1996). If both force (P) and velocity (V) is known, power output (W) can be calculated from the equation $power = force \times velocity$ ($W = P \times V$).

In order to determine whether the power output of muscle fibres from individuals with IIMs is maintained despite the disease process, we performed in vitro single fibre contractility studies to assess V_{max} and calculate power output of single muscle fibres from individuals with IIMs and healthy controls. We hypothesised that, in an attempt to maintain power output in the presence of decreased force generating capacity, V_{max} of muscle fibres from individuals with IIMs would be increased. However, since it can be anticipated that such an increase in shortening velocity will be limited by physical properties of the muscle fibres, it was furthermore hypothesised that this increase will only be able to partially compensate for the decreased force generating capacity, with a resultant decrease in power output. Our findings suggest that maximum shortening velocity is indeed increased in muscle fibres from individuals with IIMs, and power output thereby maintained or even increased.

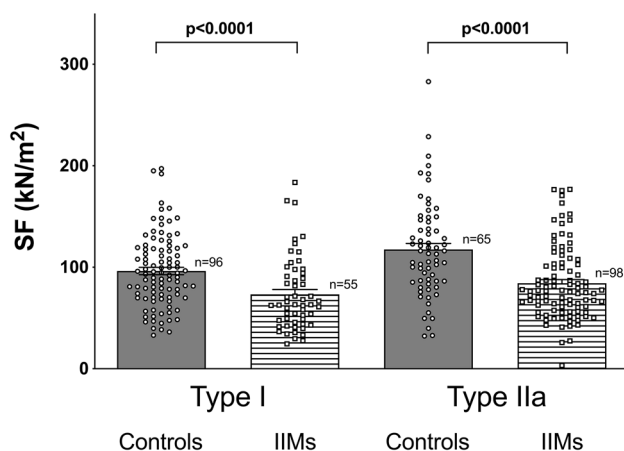


Fig. 1 Mean specific force \pm SEM of type I and IIA fibers from controls and IIMs. SF, specific force (previously published data; Henning and Kohn, 2020)

Methods

Sample collection and preparation

Muscle tissue was obtained from muscle biopsies performed for diagnostic purposes on adults with suspected IIMs. Only tissue from participants with a confirmed diagnosis of IIM, based on accepted criteria (Dalakas and Hohlfeld 2003; Liang and Needham 2011) and a response to corticosteroid treatment (initiated after the muscle biopsy) at 6 weeks after initiation, was included in the study. Individuals with inclusion body myositis were excluded, due to the different pathogenesis, clinical course, time to diagnosis, and response to treatment (Needham et al. 2008; Askanas et al. 2015; Benveniste et al. 2015). Controls consisted of healthy adults who donated muscle samples for research at the University of Cape Town Research Unit for Exercise Science and Sports Medicine.

Muscle biopsies were performed under local anaesthesia and were taken from the *vastus lateralis* muscle, either by open biopsy (IIM cases), or by means of a Bergström needle (controls). Fresh muscle specimens were immediately divided into 2–3 samples of approximately $6 \times 4 \times 4$ mm, rapidly frozen in liquid nitrogen and stored at -196 °C until analysis. Prior to analysis, each of the stored samples was thawed briefly in PBS at 37 °C for 1 min and divided into small bundles, each consisting of 20–40 muscle fibres. These bundles were then submerged into permeabilization solution containing 50% glycerol (pH 7.00), and stored at 4 °C for 24 h. After 24 h, the solution was replaced with fresh permeabilization solution and subsequently stored at -20 °C until analysis for not longer than a month.

All fibres were subjected to contractile force determination, as described previously (Henning and Kohn 2020). Subsequently, force-clamp measurements for determination of V_{max} and power output were performed on the majority of fibres ($\sim 70\%$), while the remaining fibres were used for calcium sensitivity determinations.

Determination of maximum velocity and power output

Single fibre contractility assays were performed as previously described using the Aurora Scientific 1400A permeabilised fibre test system (Aurora Scientific, Ontario, Canada) (Kohn and Noakes 2013). All measurements and pH adjustments were performed at 12 °C. The volumes and concentrations of all solutions for the single fibre contractile properties were calculated using the computer program described by Dweck et al. (2005) based on that first published by Fabiato and Fabiato (1979).

On the day of the experiment, single muscle fibres were dissected under a stereomicroscope and attached to aluminium T-clips. The fibre was then attached to the force transducer and motor and submerged in a relaxing solution containing 5 mM EDTA, 20 mM Imidazole pH 7.00, 5.08 mM ATP, with a total ionic strength of 180. The $-\log$ concentration of free ions amounted to: pMg 3.00, pCa 9.00 and pATP 2.40. After mounting, the fibre was allowed to equilibrate in the relaxing solution for approximately 5 min. During this time, the fibre was stretched to obtain a sarcomere length of between 2.40 and 2.70 μm , the optimal sarcomere length to produce maximum contractile force. Digital images were recorded at $\times 40$, $\times 100$ and $\times 200$ magnification for the determination of fibre length, diameter and sarcomere spacing, respectively, using a camera attached to the microscope. The fibre dimensions were determined using pre-calibrated software (AxioVision, Zeiss, Inc., Germany). It was assumed that fibres have a circular shape, and (cross-sectional area) CSA was determined from the diameter of the fibre using the equation $\pi [(0.8 \times \text{fibre diameter})/2]^2$, where 0.8 is to correct for an estimated 20% fibre swelling (Godt and Maughan 1977). All subsequent operations were controlled by the software program of the permeabilised single fibre system.

Once equilibrated, the fibre was transferred to a bath containing a pre-activation solution (concentrations listed as above for relaxing solution, but with 0.5 mM EDTA, 14.5 mM creatine phosphate and 200 U/ml creatine kinase) for 30 s, where after it was transferred to an activating solution. The latter contained 5 mM EDTA, 20 mM imidazole pH 7.00, 5.08 mM ATP, 14.5 mM creatine phosphate and 200 U/ml creatine kinase. The $-\log$ concentration of free ions amounted to: pMg 3.00, pCa 4.50 and pATP 2.40. This concentration has been shown to elicit maximum contraction in human muscle fibres (Bottinelli et al. 1996; Widrick et al. 1996a, b). Progress of contraction was followed on the recording program, and once a steady state of maximum force was reached, the fibre was transferred back to the relaxing solution. Force was measured in milli-Newtons (mN).

After maximum contractile force (P_0) determination, the fibre was transferred back to the relaxing solution and allowed to relax until the force returned to zero. Each fibre was then subjected to a series of isotonic force clamps to construct force–velocity curves. First, maximum activation in pCa 4.50 solution was again obtained, after which the fibre was subjected to a set of four successive force clamps, each clamp lasting 150 ms. For example, for the first force clamp set, the force was held constant at 80% of P_0 . After 150 ms, the fibre was allowed to shorten to the next pre-programmed isotonic load (55% of P_0), and the process and data recording was repeated. After a further two force clamps (30% and 10% of P_0), while the fibre was still submerged in activating solution, it was subjected to a 2 ms shortening to

50% of its original length, and then immediately re-stretched within 1 ms to its original length. This re-stretching procedure aided in preserving the fibre integrity when subjected to the next force clamp series (Brenner 1983; Gilliver et al. 2009). Following this, the fibre was transferred back to the relaxing solution and again allowed to relax and regain its initial length. The process was repeated 3 times at different isotonic loads, yielding a total of 16 force clamps in 4 sets (Table 1).

For each fibre, the shortening velocity was determined from the last 50 ms of each force clamp (length change), from which the slope was plotted against the force (% of maximum). A non-linear regression curve using the Hill-equation was fitted to the data points (GraphPad Prism v 7.0, GraphPad Software, San Diego, CA, USA). V_{max} , expressed as FL/s (fibre length per second) was calculated by extrapolating the data back to 0% force. Power output (W) was calculated from the shortening velocity and specific force parameters using the formula $power = force \times velocity$ ($W = P \times V$) and expressed as $kN/m^2 \cdot FL/s$. These values were used to construct composite velocity–force and power–force curves, and ultimately determine maximum power output (W_{max}) for each fibre, as well as optimal force (force at which W_{max} is developed, P_{opt}), expressed as percentage of P_0 ($P_{opt} \times 100\% / P_0$). Force clamp measurements were excluded from analysis if the force at maximal activation during the initial phase of the clamp dropped below 90% of P_0 . In addition, measurements obtained at less than 10% of P_0 were also excluded from the analysis. Because three of the force clamps were performed at forces less than 10% of P_0 , this yielded a maximum of 13 velocity data points per fibre. Fibres that broke during any of the force clamp sets were excluded from analysis. After measurements were performed, each fibre was placed in 90 μ l sodium dodecyl sulphate (SDS) buffer solution containing 2.5% SDS, 10% glycerol, 62.5 mM Tris, pH 6.8, and 0.1% Bromophenol Blue, and stored at $-20^\circ C$ until determination of myosin heavy chain (MyHC) composition.

Table 1 Isotonic load sequences of each set of force clamp measurements

Force clamp set	Sequence of isotonic loads (expressed as percentage of P_0)
No. 1	80, 55, 30, 10
No. 2	60, 40, 15, 2
No. 3	75, 50, 25, 6
No. 4	70, 45, 20, 4

Sets were performed in the same order (1 to 4) for each fibre. Each set consisted of four isotonic force clamps, performed in descending order. Isotonic loads are expressed as percentage of P_0 (maximum force)

Determination of single fibre MyHC isoform content

The MyHC composition of each fibre was determined by means of SDS-polyacrylamide gel electrophoresis (SDS-PAGE) based on previously described and modified protocols (Talmadge and Roy 1993; Kohn and Myburgh 2006) and utilising an 18×16 cm Hoefer SE 600 system (Hoefer, Holliston, MA, USA). On the day of the experiment, 10 μ l β -mercaptoethanol was added to each sample and the samples were heated at $95^\circ C$ for 5 min. The separating gel contained 7% acrylamide (ratio of 50 acrylamide:1 bis-acrylamide), 30% glycerol, 0.2 mM Tris buffer, pH 8.80, 0.1 mM glycine and 0.4% SDS. The stacking gel contained 4% acrylamide (50:1), 30% glycerol, 70 mM Tris buffer, pH 6.80, 0.4% SDS and 4 mM EDTA. Polymerisation was initiated using ammonium persulphate and TEMED. MyHC isoforms were identified using a homogenate that contained all three human MyHC isoforms as control in each electrophoretic run. Approximately 25 μ l of each single fibre preparation was loaded into each well, and 10 μ l of the myosin homogenate. The outer running (anode) buffer contained 50 mM Tris, 75 mM glycine and 0.05% SDS, whereas the inner running (cathode) buffer contained twice these concentrations. Prior to the electrophoretic run, 0.12% β -mercaptoethanol was added to the inner running buffer. Gels were run for 4 h at a constant 70 V, where after the voltage was increased to 275 V and electrophoresis was carried out for an additional 20 h. The gels were subsequently silver stained, scanned and the fibre type of each individual fibre determined using the loaded control as reference.

Statistical analysis

The D'Agostino and Pearson normality test was used to test data for normality of distribution. Because none of the data sets displayed a normal distribution, the non-parametric Kruskal–Wallis test with Dunn's multiple comparisons test was used to compare differences in means. Categorical data were analysed by means of the two-tailed Fisher's exact test. Statistical analysis was performed using GraphPad Prism version 7 (GraphPad Software, La Jolla, California). For all parameters, mean \pm SEM (standard error of the mean) was calculated, unless stated otherwise. Statistical significance was set at $p < 0.05$.

Ethical considerations

The Human Research Ethics Committees of both Stellenbosch University (HREC N13/10/41) and the University of Cape Town (HRECs 556/2012; 617/2014) approved the study. All participants provided written informed consent.

Results

Participants included four individuals with IIMs (all female), and four healthy controls (two male). Participant details are summarised in Table 2. The IIM group consisted of one patient with polymyositis, two with dermatomyositis, and one with necrotising autoimmune myopathy. In the IIM group, 27 of 120 (23%) fibres broke during force clamp testing (7 type I and 20 type IIA) and were excluded from the analysis, while another 2 fibres were excluded from analysis because of insufficient or unreliable data points. Overall, 91 fibres were studied from individuals with IIMs: 25 type I fibres, 58 type IIA fibres, and 8 hybrid fibres (4 I/IIA, 2 I/IX and 2 IIA/IX). In the control group, 19 from 129 fibres (15%) broke and were excluded (13 type I, 1 type I/IIA and 5 type IIA), while 9 fibres were excluded because of insufficient or unreliable data points. A total of 101 fibres, consisting of 66 type I fibres, 27 type IIA fibres, and 8 hybrid fibres (6 I/IIA, 1 I/IIA/IX, and 1 IIA/IX), were studied from the healthy control group. The difference between the two groups with respect to fibre breakage was not statistically significant. Hybrid fibres were not analysed separately due to the small numbers of these fibres in the biopsies and were excluded from further analyses.

V_{max} and power output

For type I fibres, V_{max} was 122% higher in the IIM cases (1.40 ± 0.31 FL/s vs. 0.63 ± 0.13 FL/s; $p = 0.0019$), while W_{max} was 105% higher (4.10 ± 1.00 kN/m²·FL/s vs. 2.00 ± 0.16 kN/m²·FL/s; $p =$ not significant) compared to controls. For type IIA fibres, V_{max} was 159% higher in the IIM cases (2.00 ± 0.17 FL/s vs. 0.77 ± 0.1 FL/s; $p < 0.0001$) and W_{max} was 50% higher (9.00 ± 0.64 kN/m²·FL/s vs. 6.00 ± 0.67 kN/m²·FL/s; $p =$ not significant) than control values. Figures 2 and 3 provide a visual representation of the V_{max} and W_{max} values, while Figs. 4

Table 2 Participant details. Age is reported as mean (range) in years

	Group	
	IIMs	Controls
Age	47 (26, 42, 58, 60)	33 (22, 29, 35, 44)
Gender	4F	2M, 2F
Diagnosis	1 PM, 2 DM, 1 NAM	Healthy, recreationally active
Fibre number	91 (25 type I)	101 (58 type I)

DM dermatomyositis, PM polymyositis, NAM necrotising autoimmune myopathy, F female, M male

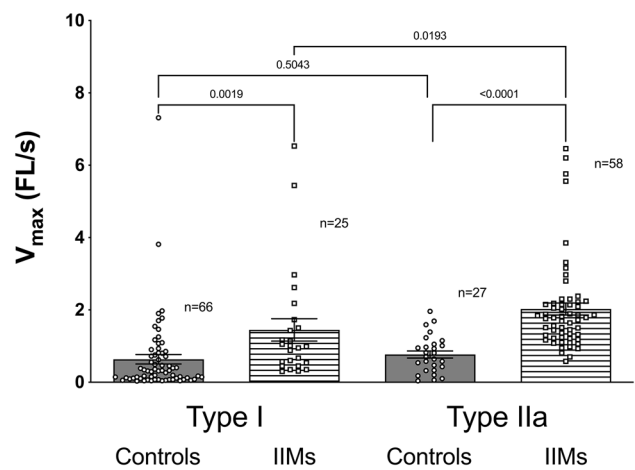


Fig. 2 V_{max} of type I and IIA fibres (means \pm SEM). V_{max} maximum shortening velocity, FL/s fibre length per second, SEM standard error of the mean

and 5 illustrate the velocity–force relationships for both fibre types.

Optimal force

W_{max} of type I fibres was obtained at $29 \pm 1\%$ and $21 \pm 1\%$ of P_0 for healthy controls and IIM cases, respectively. In the case of type IIA fibres, W_{max} was achieved at similar optimal forces as for type I fibres ($27 \pm 1\%$ and $22 \pm 1\%$ for healthy controls and IIM cases, respectively). Fibres from IIM cases, both type I and IIA, were therefore able to develop maximum power output at lower relative force, with a resultant left shift in the power–force curve (Figs. 6, 7). The difference was statistically significant for type I fibres

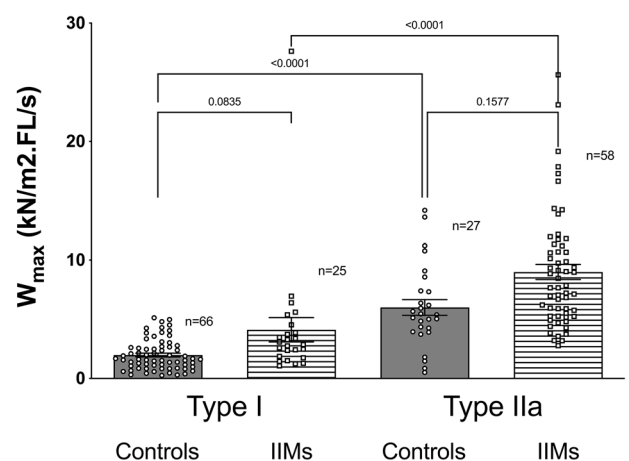


Fig. 3 Power output of type I and IIA fibres (means \pm SEM). W_{max} maximum power output, normalized to fibre CSA, SEM standard error of the mean

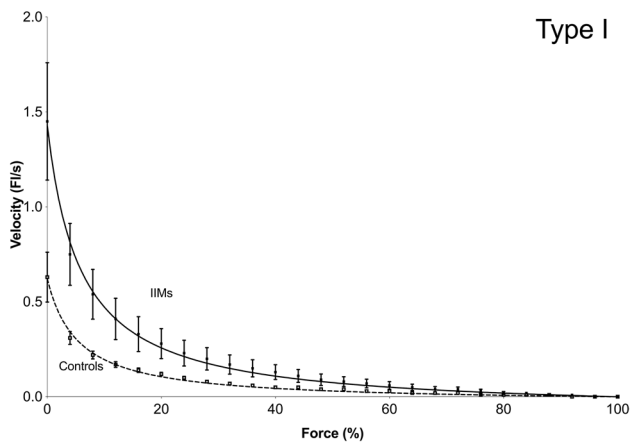


Fig. 4 Velocity–force curves of type I fibres of IIMs (solid lines) and controls (dotted lines). Force is expressed as percentage of P_0 (maximum force), velocity values are mean \pm SEM (standard error of the mean). Where the error bar would be smaller than the size of the symbol, no error bar is shown

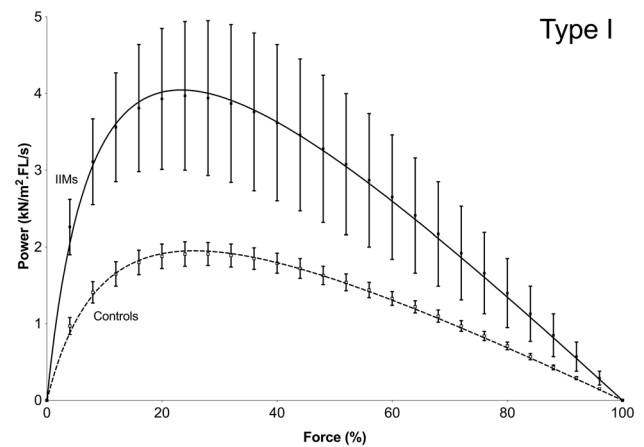


Fig. 6 Power–force curves of type I fibres of IIMs (solid lines) and controls (dotted lines). Force is expressed as percentage of P_0 (maximum force), velocity values are mean \pm SEM (standard error of the mean). Where the error bar would be smaller than the size of the symbol, no error bar is shown

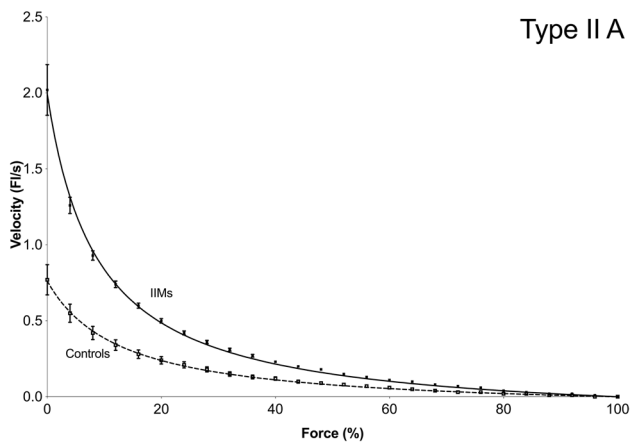


Fig. 5 Velocity–force curves of type IIA fibres of IIMs (solid lines) and controls (dotted lines). Force is expressed as percentage of P_0 (maximum force), velocity values are mean \pm SEM (standard error of the mean). Where the error bar would be smaller than the size of the symbol, no error bar is shown

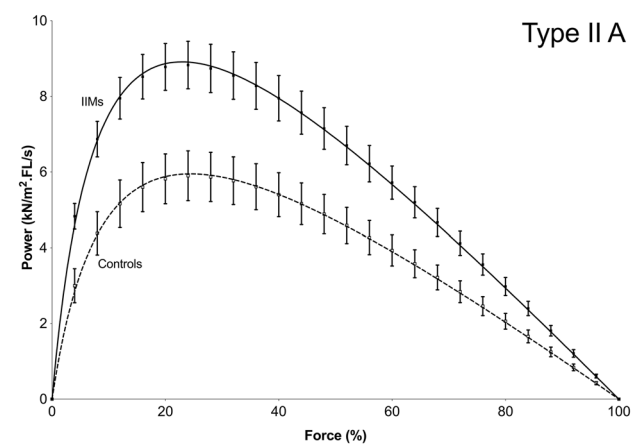


Fig. 7 Power–force curves of type IIA fibres of IIMs (solid lines) and controls (dotted lines). Force is expressed as percentage of P_0 (maximum force), velocity values are mean \pm SEM (standard error of the mean). Where the error bar would be smaller than the size of the symbol, no error bar is shown

($p < 0.0001$), but showing only a trend to be different for type IIA fibres ($p = 0.0690$).

Discussion

In order to test the hypothesis that shortening velocity and power output of muscle fibres from individuals with IIMs is maintained despite the disease process, *in vitro* single fibre studies were performed to assess force–velocity relationships and maximum shortening velocity of individual muscle fibres from individuals with IIMs and healthy controls. The findings of our study suggest significantly higher V_{max}

of fibres from individuals with IIM, while W_{max} was maintained compared to fibres from healthy controls. Muscle fibres from individuals with IIM were able to develop peak power output at lower relative force, although the difference was only statistically significant for type I fibres.

If the hypothesis that the higher V_{max} is a mechanism to maintain power output is indeed correct, the mechanism behind this compensatory response is not clear. One possible mechanism that may explain the observed findings relates to passive tension. Passive tension in muscle has traditionally been thought to arise from connective tissue between muscle fibres, as well as the non-contractile elements of the fibres (sarcolemma and sarcoplasm) (Prosser 1973). Collagen is

a prominent component of fibrosis, which is often seen in IIMs (Dubowitz et al. 2013). Although it often becomes visible on routine histological examination only in more advanced disease, it is likely to be present from early in the disease process. Indeed, collagen appears to be one of the main contributors to passive tension originating from connective tissue in cardiac muscle (Granzier and Irving 1995), and is likely to have a similar effect in skeletal muscle. Although collagen is a component of the endomysium, skinned fibres contain small amounts of collagen. In a recent study of skinned fibres from *muscular dystrophy with myositis (mdm)* mice, mutant fibres contained $7.9 \pm 3.5\%$ collagen vs. $0.3 \pm 0.1\%$ in control fibres (Powers et al. 2017). This finding suggests that collagen may contribute to mechanics at a fibre level, even though it is a component of the extracellular matrix. Recently, evidence has emerged that an important component of passive tension arises from the sarcomere (Magid and Law 1985), in particular the protein titin (Maruyama et al. 1976; Wang et al. 1979; Horowitz 1999). Furthermore, single muscle fibre studies in facioscapulohumeral dystrophy (FSHD) have shown that both passive force and calcium sensitivity were increased, while myofilament lattice spacing was decreased (suggesting titin stiffening) (Lassche et al. 2013). The authors hypothesised that titin stiffening is a mechanism to compensate for muscle weakness in FSHD by increasing the calcium sensitivity of the sarcomeres. Although the pathogenesis of FSHD and IIMs is different, it is possible that similar compensatory mechanisms exist across the spectrum of muscle disorders, including the IIMs. Interestingly, increased V_{\max} has also been illustrated in nervous system conditions without direct muscle fibre damage, such as spinal cord injury and amyotrophic lateral sclerosis (Krivickas et al. 2002; Malisoux et al. 2007), as well as chronic unloading of muscle, like prolonged bed rest (Yamashita-Goto et al. 2001; D'Antona et al. 2003) and space flight (Widrick et al. 1999). In the case of prolonged bed rest, the increased shortening velocity was associated with a decrease in maximum contractile force, whereas contractile force was not affected in spinal cord injury. Moreover, in contrast to the findings in FSHD (Lassche et al. 2013), passive tension was not increased in muscle fibres from individuals with spinal cord injury. Matters are further complicated by reports of increased shortening velocity in response to certain types of strengthening exercise, a contrasting physiological stimulus in terms of muscle activation (Malisoux et al. 2006).

In addition to an increase in passive tension, there are other potential mechanisms to increase shortening velocity which require consideration. The combination of reduced force and increased shortening velocity could potentially be caused by a process that increases the rate of crossbridge detachment, as has been shown with increased ADP or decreased ATP concentrations (Cooke and Bialek 1979;

Cooke and Pate 1985; Seow and Ford 1997). Alteration of sarcomeric protein content or structure (via e.g. post-translational modification) could theoretically have a similar effect. For example, differences in myosin light chain (MyLC) isoform content and phosphorylation could theoretically affect shortening velocity. In the rat, variability of maximum shortening velocity in fibres with similar MyHC content is related to MyLC isoform content, with higher velocity correlating with a higher alkali MLC3f content (Bottinelli et al. 1994; Bottinelli and Reggiani 1995). However, a similar effect of the MyLC isoform on shortening velocity in human fibres has not been demonstrated in a number of conditions, including normal physiological conditions (Larsson and Moss 1993), space flight (Widrick et al. 1999), endurance training (Widrick et al. 1996a, b), and aging (D'Antona et al. 2003). Interestingly, in rats, the MyHC isoform that seems most sensitive to MyLC isoform variation is IIB. While this is the predominant isoform in rats, it is absent or only minimally expressed in human skeletal muscle (Harrison et al. 2011), which may partially explain the fact that V_{\max} in humans appeared to be insensitive to MyLC variation. Post-translational modification of myosin, in particular phosphorylation of regulatory MyLC, also does not appear to influence V_{\max} (Persechini et al. 1985; Sweeney and Kushmerick 1985). The influence of the mechanical performance of myosin molecules on shortening velocity should also be considered. The sliding velocity of actin over myosin at zero load is dependent on the rate of cross-bridge turnover, and potentiation of this interaction could theoretically influence shortening velocity. The velocity at which myosin translocates actin filaments can be measured by means of the in vitro motility assay (IVMA). This method allows direct observation of the movement of a single fluorescently labelled actin filament as it glides over a myosin-coated glass surface, and eliminates passive tension from the experimental set-up (Warshaw 1996). To date, no IVMA investigations of muscle fibres from individuals with IIMs have been performed but decreased sliding velocities have been demonstrated in diaphragmatic and cardiac muscle of dystrophic mice (Coirault et al. 2002; Wagner et al. 2012). In addition, although immobilization was associated with increased maximum shortening velocity, it did not affect the actin sliding velocity as assessed by IVMA (D'Antona et al. 2003). This assay would be invaluable to further investigate the mechanisms behind the increased V_{\max} observed in the current study, as a normal motility assay will support the contribution of passive tension, and vice versa.

An interesting finding of this study is that power output of fibres from individuals with IIM is at least maintained, suggesting that the increase in maximum shortening velocity is of a sufficient magnitude to compensate for the decrease in force generation. Despite this response, clinical weakness still develops, emphasising the relative importance of

force production compared to shortening velocity in muscle function. It should also be noted that, despite the theoretical advantages of increased shortening velocity, it is entirely possible that the observed response is an unintended consequence, rather than a true compensatory mechanism. In order to clarify this, repeat single fibre force and velocity measurements, performed after resolution of weakness with treatment, will be informative. Decreased or normalisation of V_{\max} , in parallel with increase or normalisation of specific force, will support the hypothesis of a compensatory mechanism.

This study has a number of potential limitations. Firstly, it could be argued that the different disease entities included in the IIM group all have different pathological mechanisms. While this may be true, they also share a number of characteristics, some of which may be relevant to the context of the current study and provide sufficient justification to “lump” these entities together for the purpose of this investigation, as discussed above. Although the inclusion of sufficient numbers of individuals with each of the separate disease entities would be ideal, such investigations are limited by the rarity of the disorders and the time-consuming nature of the experiments. A second limitation is incomplete matching for sex and age in the control group. Two of the four controls were male, while all four IIM cases were female, and the mean age in the IIM group was substantially higher (Table 2). However, this is unlikely to have influenced the main results, as it has been shown that greater strength in men is primarily related to larger diameter of muscle fibres (Miller et al. 1993), and both normalised force and normalised peak power are similar in men and women, as well as in the young and old (Trappe et al. 2003). In addition, it should be noted that a few studies suggested a decrease and not an increase in maximum shortening velocity with age (Larsson et al. 1997; D’Antona et al. 2003). The higher median age in the IIM group in this study therefore makes the findings even more convincing. Lastly, potential mechanisms to explain the findings were not explored in this study.

In conclusion, the findings of this study suggest that compensatory responses to maintain power output occur in muscle of individuals with IIMs. These responses include increased maximum shortening velocity and appear to be present in both type I and IIA fibres. The mechanism underlying this response is unclear, but may be related to increased passive tension, increased rate of cross-bridge turnover, or a different, as yet unidentified factor.

Supplementary Information The online version contains supplementary material available at <https://doi.org/10.1007/s10974-022-09638-w>.

Author contributions The experimental work was performed in the MyoLab of Professor Kohn, Division of Exercise Science and Sports Medicine, University of Cape Town. FH and TAK conceptualised and designed the study. FH performed the acquisition, analysis, and

interpretation of the data, and drafted and revised the manuscript. TAK revised the manuscript. All authors approved the final version and takes full accountability for the accuracy of the manuscript content. All listed authors qualify for authorship.

Data availability The datasets generated during and/or analysed during the current study are available from the corresponding author on reasonable request.

Declarations

Conflict of interest All authors confirm no competing interests or conflicting interests.

References

- Askanas V, Engel WK, Nogalska A (2015) Sporadic inclusion-body myositis: a degenerative muscle disease associated with aging, impaired muscle protein homeostasis and abnormal mitophagy. *Biochim Biophys Acta* 1852(4):633–643. <https://doi.org/10.1016/j.bbadis.2014.09.005>
- Benveniste O, Stenzel W, Hilton-Jones D, Sandri M, Boyer O, van Engelen BG (2015) Amyloid deposits and inflammatory infiltrates in sporadic inclusion body myositis: the inflammatory egg comes before the degenerative chicken. *Acta Neuropathol* 129(5):611–624. <https://doi.org/10.1007/s00401-015-1384-5>
- Bottinelli R, Reggiani C (1995) Force–velocity properties and myosin light chain isoform composition of an identified type of skinned fibres from rat skeletal muscle. *Pflugers Arch* 429(4):592–594
- Bottinelli R, Reggiani C (2000) Human skeletal muscle fibres: molecular and functional diversity. *Prog Biophys Mol Biol* 73(2–4):195–262
- Bottinelli R, Betto R, Schiaffino S, Reggiani C (1994) Unloaded shortening velocity and myosin heavy chain and alkali light chain isoform composition in rat skeletal muscle fibres. *J Physiol* 478(Pt 2):341–349
- Bottinelli R, Canepari M, Pellegrino MA, Reggiani C (1996) Force–velocity properties of human skeletal muscle fibres: myosin heavy chain isoform and temperature dependence. *J Physiol* 495(Pt 2):573–586
- Brenner B (1983) Technique for stabilizing the striation pattern in maximally calcium-activated skinned rabbit psoas fibers. *Biophys J* 41(1):99–102. [https://doi.org/10.1016/s0006-3495\(83\)84411-7](https://doi.org/10.1016/s0006-3495(83)84411-7)
- Coirault CL, Lambert F, Pourny J-C, Lecarpentier Y (2002) Velocity of actomyosin sliding in vitro is reduced in dystrophic mouse diaphragm. *Am J Respir Crit Care Med* 165(2):250–253. <https://doi.org/10.1164/ajrccm.165.2.2105088>
- Coley W, Rayavarapu S, Pandey GS, Sabina RL, Van der Meulen JH, Ampong B, Wortmann RL, Rawat R, Nagaraju K (2012) The molecular basis of skeletal muscle weakness in a mouse model of inflammatory myopathy. *Arthritis Rheumatol* 64(11):3750–3759.
- Cooke R, Bialek W (1979) Contraction of glycerinated muscle fibers as a function of the ATP concentration. *Biophys J* 28(2):241–258. [https://doi.org/10.1016/S0006-3495\(79\)85174-7](https://doi.org/10.1016/S0006-3495(79)85174-7)
- Cooke R, Pate E (1985) The effects of ADP and phosphate on the contraction of muscle fibers. *Biophys J* 48(5):789–798. [https://doi.org/10.1016/S0006-3495\(85\)83837-6](https://doi.org/10.1016/S0006-3495(85)83837-6)
- Dalakas MC, Hohlfeld R (2003) Polymyositis and dermatomyositis. *Lancet* 362(9388):971–982. [https://doi.org/10.1016/S0140-6736\(03\)14368-1](https://doi.org/10.1016/S0140-6736(03)14368-1)
- D’Antona G, Pellegrino MA, Adami R, Rossi R, Carlizzi CN, Canepari M, Saltin B, Bottinelli R (2003) The effect of ageing and immobilization on structure and function of human skeletal muscle fibres.

- J Physiol 552(Pt 2):499–511. <https://doi.org/10.1113/jphysiol.2003.046276>
- Dubowitz V, Oldfors A, Sewry CA (2013) Muscle biopsy: a practical approach. Elsevier Health Sciences, Philadelphia
- Dweck D, Reyes-Alfonso A Jr, Potter JD (2005) Expanding the range of free calcium regulation in biological solutions. *Anal Biochem* 347(2):303–315. <https://doi.org/10.1016/j.ab.2005.09.025>
- Edman KA (1979) The velocity of unloaded shortening and its relation to sarcomere length and isometric force in vertebrate muscle fibres. *J Physiol* 291:143–159
- Fabiato A, Fabiato F (1979) Calculator programs for computing the composition of the solutions containing multiple metals and ligands used for experiments in skinned muscle cells. *J Physiol (Paris)* 75(5):463–505
- Fink RH, Stephenson DG, Williams DA (1990) Physiological properties of skinned fibres from normal and dystrophic (Duchenne) human muscle activated by Ca^{2+} and Sr^{2+} . *J Physiol* 420:337–353
- Gilliver SF, Degens H, Rittweger J, Sargeant AJ, Jones DA (2009) Variation in the determinants of power of chemically skinned human muscle fibres. *Exp Physiol* 94(10):1070–1078. <https://doi.org/10.1113/expphysiol.2009.048314>
- Godt RE, Maughan DW (1977) Swelling of skinned muscle fibers of the frog. Experimental observations. *Biophys J* 19(2):103–116. [https://doi.org/10.1016/s0006-3495\(77\)85573-2](https://doi.org/10.1016/s0006-3495(77)85573-2)
- Granzier HL, Irving TC (1995) Passive tension in cardiac muscle: contribution of collagen, titin, microtubules, and intermediate filaments. *Biophys J* 68(3):1027–1044. [https://doi.org/10.1016/s0006-3495\(95\)80278-x](https://doi.org/10.1016/s0006-3495(95)80278-x)
- Harrison BC, Allen DL, Leinwand LA (2011) I1b or not I1b? Regulation of myosin heavy chain gene expression in mice and men. *Skelet Muscle* 1:5
- Henning F, Kohn TA (2020) An exploratory study of contractile force production in muscle fibers from patients with inflammatory myopathies. *Muscle Nerve* 62(2):284–288. <https://doi.org/10.1002/mus.26904>
- Hill AV (1938) The heat of shortening and the dynamic constants of muscle. *Proc R Soc Lond B* 126(843):136–195. <https://doi.org/10.1098/rspb.1938.0050>
- Himori K, Ashida Y, Tatebayashi D, Abe M, Saito Y, Chikenji T, Westerblad H, Andersson DC, Yamada T (2021) Eccentric resistance training ameliorates muscle weakness in a mouse model of idiopathic inflammatory myopathies. *Arthritis Rheumatol* 73(5):848–857. <https://doi.org/10.1002/art.41594>
- Horowitz R (1999) The physiological role of titin in striated muscle. *Rev Physiol Biochem Pharmacol* 138:57–96. <https://doi.org/10.1007/BFb0119624>
- Kluger BM, Krupp LB, Enoka RM (2013) Fatigue and fatigability in neurologic illnesses: proposal for a unified taxonomy. *Neurology* 80(4):409–416. <https://doi.org/10.1212/WNL.0b013e31827f07be>
- Kohn TA, Myburgh KH (2006) Electrophoretic separation of human skeletal muscle myosin heavy chain isoforms: the importance of reducing agents. *J Physiol Sci* 56(5):355–360. <https://doi.org/10.2170/physiolsci.RP007706>
- Kohn TA, Noakes TD (2013) Lion (*Panthera leo*) and caracal (*Caracal caracal*) type I1x single muscle fibre force and power exceed that of trained humans. *J Exp Biol* 216(Pt 6):960–969. <https://doi.org/10.1242/jeb.078485>
- Krivickas LS, Ansvet T, Suh D, Frontera WR (2000) Contractile properties of single muscle fibers in myotonic dystrophy. *Muscle Nerve* 23(4):529–537. [https://doi.org/10.1002/\(SICI\)1097-4598\(200004\)23:4<529::AID-MUS11%3e3.0.CO;2-Y](https://doi.org/10.1002/(SICI)1097-4598(200004)23:4<529::AID-MUS11%3e3.0.CO;2-Y)
- Krivickas LS, Yang JI, Kim SK, Frontera WR (2002) Skeletal muscle fiber function and rate of disease progression in amyotrophic lateral sclerosis. *Muscle Nerve* 26(5):636–643. <https://doi.org/10.1002/mus.10257>
- Krivickas LS, Amato AA, Krishnan G, Murray AV, Frontera WR (2005) Preservation of in vitro muscle fiber function in dermatomyositis and inclusion body myositis: a single fiber study. *Neuromuscul Disord* 15(5):349–354. <https://doi.org/10.1016/j.nmd.2005.01.011>
- Larsson L, Moss RL (1993) Maximum velocity of shortening in relation to myosin isoform composition in single fibres from human skeletal muscles. *J Physiol* 472:595–614
- Larsson L, Li X, Frontera WR (1997) Effects of aging on shortening velocity and myosin isoform composition in single human skeletal muscle cells. *Am J Physiol* 272(2 Pt 1):C638–649. <https://doi.org/10.1152/ajpcell.1997.272.2.C638>
- Lassche S, Stienen GJ, Irving TC, van der Maarel SM, Voermans NC, Padberg GW, Granzier H, van Engelen BG, Ottenheijm CA (2013) Sarcomeric dysfunction contributes to muscle weakness in facioscapulohumeral muscular dystrophy. *Neurology* 80:733–737
- Liang C, Needham M (2011) Necrotizing autoimmune myopathy. *Curr Opin Rheumatol* 23(6):612–619. <https://doi.org/10.1097/BOR.0b013e32834b324b>
- Magid A, Law DJ (1985) Myofibrils bear most of the resting tension in frog skeletal muscle. *Science* 230(4731):1280–1282
- Malisoux L, Francaux M, Nielens H, Theisen D (2006) Stretch-shortening cycle exercises: an effective training paradigm to enhance power output of human single muscle fibers. *J Appl Physiol* (1985) 100(3):771–779. <https://doi.org/10.1152/japplphysiol.01027.2005>
- Malisoux L, Jamart C, Delplace K, Nielens H, Francaux M, Theisen D (2007) Effect of long-term muscle paralysis on human single fiber mechanics. *J Appl Physiol* (1985) 102(1):340–349. <https://doi.org/10.1152/japplphysiol.00609.2006>
- Maruyama K, Natori R, Nonomura Y (1976) New elastic protein from muscle. *Nature* 262(5563):58–60. <https://doi.org/10.1038/262058a0>
- Mastaglia FL, Garlepp MJ, Phillips BA, Zilko PJ (2003) Inflammatory myopathies: clinical, diagnostic and therapeutic aspects. *Muscle Nerve* 27(4):407–425. <https://doi.org/10.1002/mus.10313>
- Miller AE, MacDougall JD, Tarnopolsky MA, Sale DG (1993) Gender differences in strength and muscle fiber characteristics. *Eur J Appl Physiol Occup Physiol* 66(3):254–262
- Needham M, James I, Corbett A, Day T, Christiansen F, Phillips B, Mastaglia FL (2008) Sporadic inclusion body myositis: phenotypic variability and influence of HLA-DR3 in a cohort of 57 Australian cases. *J Neurol Neurosurg Psychiatry* 79(9):1056–1060. <https://doi.org/10.1136/jnnp.2007.138891>
- Persechini A, Stull JT, Cooke R (1985) The effect of myosin phosphorylation on the contractile properties of skinned rabbit skeletal muscle fibers. *J Biol Chem* 260(13):7951–7954
- Powers K, Joumaa V, Jinha A, Moo EK, Smith IC, Nishikawa K, Herzog W (2017) Titin force enhancement following active stretch of skinned skeletal muscle fibres. *J Exp Biol* 220(Pt 17):3110–3118. <https://doi.org/10.1242/jeb.153502>
- Prosser CL (1973) Comparative animal physiology. W.B. Saunders, Philadelphia
- Seow CY, Ford LE (1997) Exchange of ATP for ADP on high-force cross-bridges of skinned rabbit muscle fibers. *Biophys J* 72(6):2719–2735. [https://doi.org/10.1016/S0006-3495\(97\)78915-X](https://doi.org/10.1016/S0006-3495(97)78915-X)
- Sweeney HL, Kushmerick MJ (1985) Myosin phosphorylation in permeabilized rabbit psoas fibers. *Am J Physiol* 249(3 Pt 1):C362–365. <https://doi.org/10.1152/ajpcell.1985.249.3.C362>
- Talmadge RJ, Roy RR (1993) Electrophoretic separation of rat skeletal muscle myosin heavy-chain isoforms. *J Appl Physiol* (1985) 75(5):2337–2340. <https://doi.org/10.1152/jappl.1993.75.5.2337>
- Trappe S, Gallagher P, Harber M, Carrithers J, Fluckey J, Trappe T (2003) Single muscle fibre contractile properties in young and old men and women. *J Physiol* 552(Pt 1):47–58. <https://doi.org/10.1113/jphysiol.2003.044966>

- Wagner S, Knipp S, Weber C, Hein S, Schinkel S, Walther A, Bekeredjian R, Müller OJ, Friedrich O (2012) The heart in Duchenne muscular dystrophy: early detection of contractile performance alteration. *J Cell Mol Med* 16(12):3028–3036. <https://doi.org/10.1111/j.1582-4934.2012.01630.x>
- Wang K, McClure J, Tu A (1979) Titin: major myofibrillar components of striated muscle. *Proc Natl Acad Sci USA* 76(8):3698–3702. <https://doi.org/10.1073/pnas.76.8.3698>
- Warshaw DM (1996) The in vitro motility assay: a window into the myosin molecular motor. *Physiology* 11(1):1–7. <https://doi.org/10.1152/physiologyonline.1996.11.1.1>
- Widrick JJ, Trappe SW, Blaser CA, Costill DL, Fitts RH (1996a) Isometric force and maximal shortening velocity of single muscle fibers from elite master runners. *Am J Physiol* 271(2 Pt 1):C666–675
- Widrick JJ, Trappe SW, Costill DL, Fitts RH (1996b) Force–velocity and force–power properties of single muscle fibers from elite master runners and sedentary men. *Am J Physiol* 271(2 Pt 1):C676–683
- Widrick JJ, Knuth ST, Norenberg KM, Romatowski JG, Bain JL, Riley DA, Karhanek M, Trappe SW, Trappe TA, Costill DL, Fitts RH (1999) Effect of a 17 day spaceflight on contractile properties of human soleus muscle fibres. *J Physiol* 516(Pt 3):915–930
- Yamashita-Goto K, Okuyama R, Honda M, Kawasaki K, Fujita K, Yamada T, Nonaka I, Ohira Y, Yoshioka T (2001) Maximal and submaximal forces of slow fibers in human soleus after bed rest. *J Appl Physiol* (1985) 91(1):417–424. <https://doi.org/10.1152/jappl.2001.91.1.417>

Publisher's Note Springer Nature remains neutral with regard to jurisdictional claims in published maps and institutional affiliations.

Springer Nature or its licensor (e.g. a society or other partner) holds exclusive rights to this article under a publishing agreement with the author(s) or other rightsholder(s); author self-archiving of the accepted manuscript version of this article is solely governed by the terms of such publishing agreement and applicable law.